Neuropsychiatric Disease and Treatment

Dovepress
Taylor & Francis Group

Open Access Full Text Article

ORIGINAL RESEARCH

Construction and Brain Validation of circRNAs-miRNAs-mRNAs Regulatory Axis in Early-Onset Schizophrenia

Xiuping Zhang[1,2,*], Zexuan Li[3,4,*], Ruiting Li[5,*], Xinxia Wang[1], Huanghui Liu[1], Xinzhe Du[1,4], Yao Gao[1,4], Sha Liu[1,4], Yong Xu[1,3,4]

[1]Department of Psychiatry, Shanxi Medical University, Taiyuan, People's Republic of China; [2]Department of Neurology, Second Hospital of Shanxi Medical University, Taiyuan, People's Republic of China; [3]Department of Psychiatry, The Eighth Affiliated Hospital, Sun Yat-sen University, Shenzhen, People's Republic of China; [4]Shanxi Key Laboratory of Artificial Intelligence Assisted Diagnosis and Treatment for Mental Disorder, First Hospital of Shanxi Medical University, Taiyuan, People's Republic of China; [5]Department of Pain Management, Taiyuan Central Hospital, Taiyuan, People's Republic of China

*These authors contributed equally to this work

Correspondence: Yong Xu; Sha Liu, Department of Psychiatry, Shanxi Medical University, Taiyuan, People's Republic of China, Email xuyongsmu@vip.163.com; liusha198411 4@163.com

Background: High rates of misdiagnosis and missed diagnosis of schizophrenia highlight the urgent need for objective diagnostic indicators. Previous studies showed that microRNAs and circular RNAs are potential candidates. This study aimed to investigate the regulatory patterns and brain validation of circular RNAs-microRNAs-messenger RNAs in early-onset schizophrenia.

Methods: Differentially expressed circular RNAs and microRNAs were identified in blood samples from 32 patients with early-onset schizophrenia and 29 healthy controls. Circular RNAs were confirmed to possess circular structures. The interactions among circular RNAs, microRNAs, and messenger RNAs were examined using dual-luciferase reporter assays. The circRNA of interest was knocked down and overexpressed in the SH-SY5Y cell line to evaluate changes in gene expression. Brain validation of the axis was performed in animal models.

Results: Compared with healthy controls, 8 circular RNAs and 3 microRNAs exhibited significant and stable differential expression, with 6 of the 8 circular RNAs confirmed to have circular structures. Hsa-circ-0000713 was identified as containing the response element for hsa-miR-370-3p, which targeted ANK3 and MGLL. Hsa-circ-0000713 acted as a sponge, mitigating the inhibitory effects of hsa-miR-370-3p on ANK3 and MGLL. The expression patterns of this axis in the prefrontal cortex were consistent with those observed in peripheral blood samples from clinical patients.

Conclusion: This study identified a specific multi-molecular axis in early-onset schizophrenia, wherein hsa-circ-0000713 functioned as a sponge to reduce the inhibitory effects of hsa-miR-370-3p on ANK3 and MGLL. This axis may contribute to the pathogenesis of early-onset schizophrenia by mediating abnormalities in prefrontal cortex development.

Keywords: early-onset schizophrenia, circRNAs, miRNAs, mRNAs, multi-molecular axis, brain validation

Introduction

Schizophrenia (SZ) is a chronic, severe, and disabling mental disorder, with approximately 5–6% of patients experiencing suicide.[1,2] Its diagnosis relies primarily on clinical symptoms, which exhibit high heterogeneity, leading to challenges in accurate identification, as well as high rates of misdiagnosis and missed diagnosis.[3,4] This underscores the urgent need for objective diagnostic indicators, including potential physiological, biochemical, and pathological markers.

MicroRNAs (miRNAs) regulate gene expression post-transcriptionally by binding complementarily to the 3′-untranslated regions (3′UTRs) of target messenger RNAs (mRNAs), resulting in mRNA degradation or translation inhibition.[5] Circular RNAs (circRNAs) is a type of closed circular non-coding RNA that lacks the 5′ cap structure and the 3′ tail. Due to their resistance to RNA exonucleases, they exhibit high stability and a long half-life. Highly conserved circRNAs are widely

Received: 9 February 2025
Accepted: 8 July 2025
Published: 22 July 2025

present in human blood, urine, amniotic fluid, and various tissues and organs.[6–8] Evidence has suggested that circRNAs in the dorsolateral prefrontal cortex may be associated with neuroinflammation and other stress response mechanisms related to SZ.[9] As "sponge molecules" for miRNAs, circRNAs can partially alleviate the inhibitory effects of miRNAs on mRNAs.[10,11]

For example, ciRS-7 contains multiple miR-7 binding sites, which can effectively inhibit the activity of miR-7 and upregulate the expression of related mRNAs, forming the circRNA-miRNA-mRNA regulatory axis.[12] In SZ, the differentially expressed circRNA chr5:6917537–6917487 carries the target sequences of miR-34a-5p and miR-449a, which have been confirmed to be closely related to the prognosis.[13] MiRNAs have been shown to play a key role in brain development by regulating signaling pathways critical for synaptic formation, neuronal plasticity, nerve growth, and memory processes.[14] Perkins et al identified 16 miRNAs with abnormal expression in the dorsolateral prefrontal cortex (BA9 region) of SZ patients.[15] Dysregulated circRNAs and miRNAs thus represent promising candidates as objective diagnostic indicators for SZ.[16–19]

In this study, early-onset schizophrenia (EOS) was chosen as the research focus to reduce clinical heterogeneity and minimize the influence of social factors.[20,21] Based on our previous high-throughput sequencing datasets of circRNAs and miRNAs in EOS, selected circRNAs and miRNAs were validated. Interactions among circRNAs, miRNAs, and mRNAs were explored to construct a regulatory axis, which was further validated in two SZ animal models. This integration of circRNAs, miRNAs, and mRNAs provides valuable insights into the pathogenesis of EOS and offers a foundation for developing objective diagnostic approaches for EOS.

Materials and Methods

Participants

Patients with EOS were enrolled between October 2021 and August 2023 in the Department of Psychiatry, First Hospital of Shanxi Medical University (China Clinical Trial Registry: ChiCTR1900025838). Patients with an onset before the age of 18 were diagnosed with SZ by two psychiatrists using the Diagnostic and Statistical Manual of Mental Disorders, Fifth Edition (DSM-5).[22] Peripheral blood samples were collected from 32 patients with EOS and 29 age- and sex-matched healthy controls (HCs) after fasting in the morning and stored at −80°C. All procedures were conducted in accordance with relevant regulations and guidelines following informed consent from participants.

Quantitative Real-Time Polymerase Chain Reaction

Total RNA and miRNAs were reverse-transcribed into complementary DNA (cDNA) using mRNA reverse transcription kits (AG11728) and miRNA reverse transcription kits (AG11745) from Hunan Ecorui Biological Engineering Co., Ltd., China. Quantitative real-time polymerase chain reaction (qRT-PCR) was performed with the qPCR reagent (AG11739) on a Real-Time PCR Detection System (ABI). GAPDH and U6 served as internal controls. Data were analyzed using the $2^{-\Delta\Delta Ct}$ method. The sequences of the primers are listed in Supplementary Table S1.

Sanger Sequencing and RNase R Resistance Assay

Sanger sequencing involved: 1) Amplifying the target circular junction using PCR. 2) Identifying the expected band size through gel electrophoresis. 3) Performing Sanger sequencing on the purified PCR product. The RNase R resistance assay involved: 1) Treating RNA samples containing the target circRNAs and controls with RNase R. 2) Amplifying the remaining circRNAs in treated RNA samples using PCR. Positive results in the treated samples and negative results in the controls confirmed the presence of circRNAs.

Dual-Luciferase Reporter Assay

To construct the pmirGLO carrier, the target fragment was synthesized, and double enzyme digestion was performed by adding endonuclease to the empty carrier. The results were analyzed using BLAST sequence comparison and identified as target genes in Supplementary Table S2. Low-endotoxin plasmid extraction was conducted following the manufacturer's protocol. Prior to transfection, 3–5 × 10^5 HEK293T cells obtained from Shanxi Key Laboratory of Carcinogenesis and Translational Research on Esophageal Cancer per well were seeded in a 6-well plate and cultured at 37°C with 5% CO_2.

Transfection was performed 48 hours later. Each pairing relationship and experimental group had three replicate wells, as did the control group. Target paired genes were co-transfected into HEK293T cells using TransIntro® EL Transfection Reagent (Beijing All-Style Gold Biotechnology Co., Ltd). Luciferase activities were measured using the Dual Luciferase Assay System (Promega, Madison, WI, USA).

Overexpression and Knockdown of Hsa-Circ-0000713

Overexpression plasmids and two small interfering RNAs (siRNAs) targeting hsa-circ-0000713 were constructed. After identification of the target gene, low-endotoxin plasmid extraction was performed according to the instructions of the low-endotoxin plasmid extraction kit (Magen) and stored at −20°C. The sequences of si-1-hsa-circ-0000713 and si-2-hsa-circ-0000713 are provided in Supplementary Table S3. These constructs were transfected into the SH-SY5Y human neuroblastoma cell line obtained from EK-Bioscience. Changes in the expression of hsa-circ-0000713, hsa-miR-370-3p, and the target genes ANK3 and MGLL were detected using qRT-PCR. The primers used are listed in Supplementary Table S4.

Animal Model

Fifteen pregnant Sprague-Dawley (SD) rats were maintained at a temperature of 24°C and a humidity of 60%.[23] They were randomly divided into three groups: HC (n = 5), methylazoxymethanol acetate (MAM, n = 5), and polyinosinic-polycytidylic acid (Poly I:C, n = 5). MAM was intraperitoneally injected at 21 mg/kg on gestational day 17.[24,25] Poly I:C was administered via tail vein injection at 10 mg/kg on gestational day 14.[26] Offspring were weighed, and behavioral testing began at five weeks of age (PND35). Behavioral assessments included the open field test, novel object recognition, and Y-maze alternating behavior test to evaluate modeling effects. Frontal lobe samples were collected to validate the circRNA-miRNA-mRNA regulatory axis in the brain.

Animal Behavior Protocol

Open Field Test

The animals were brought into the laboratory 24 hours in advance, and the 75% ethanol solution was used to clean the feces and urine left behind by the animal from the previous experiment. Placed the experimental animal in the central area of the open field, opened the animal behavior analysis software Spain Pan Lab Smart 3.0 and automatically recorded the trajectory map of the rat activities within 5 minutes.

Novel Object Recognition

The animal was allowed to freely move around in the square open box without objects for 5 minutes. Then two objects with the same fixed position were placed in the box. The animal was placed with its back facing the objects and placed in the device at an equal distance from the objects for 5 minutes of free exploration. The time to explore the two objects was recorded. One of the two identical objects was replaced with a different object. The rat was placed in the device with its back facing away from the object and allowed to freely explore for 5 minutes from an equal distance from the object. The time to explore the two objects was recorded.

Y-maze Alternating Behavior Test

The experimental device consisted of three identical black iron plate arms radiating from a central triangle and spaced 120° apart from each other. The experimental animal was placed at the end of the starting arm, facing the central triangle, and the time spent in each arm and the rate of alternating exploration during the 8-minute free exploration period were recorded.[27–29]

Statistical Analysis

Data were analyzed using SPSS 23.0 (Statistical Product and Service Solutions). An unpaired *t*-test was applied for normally distributed data, while the non-parametric Mann–Whitney test was used for non-normally distributed data. For comparisons among three or more groups, one-way analysis of variance (ANOVA) was used if the data satisfied normality and homogeneity of variance assumptions. If these assumptions were not met, the non-parametric Kruskal–Wallis test was employed. A value of $P<0.05$ was considered statistically significant.

Results

Expressed Verification of Screened circRNAs and miRNAs in Early-Onset Schizophrenia

Based on functional enrichment analysis, 10 circRNAs and 3 miRNAs were screened from our previous high-throughput sequencing datasets of circRNAs and miRNAs in EOS.[22] The expression trends of these circRNAs and miRNAs were validated in the current cohort of 32 EOS patients and 29 HCs. There were no statistically significant differences in age (Mann–Whitney *U*-test, *P*=0.5239), educational years (Mann–Whitney *U*-test, *P*=0.2100), and gender (chi-square test, *P*=0.9326) between the EOS and HCs groups (See the detailed statistical analysis results in Supplementary Table S5).

Compared with HCs, chr11:33307959–33309057+, chr17:26490569–26499644+, chr16:23999829–24046868+, chr19:-41847788–41848152-, and chr7:152007051–152012423- were significantly downregulated, while chr12:46622936–-46648719-, chr18:44526020–44526886+, and chr16:68224671–68225678+ were significantly upregulated in EOS (Figure 1A–C). In contrast, chr16:85667520–85667738- and chr12:69044180–69048032+ exhibited lower expression levels in EOS compared to HCs, but the differences were not statistically significant (Figure 1D). Additionally, hsa-miR-335-3p, hsa-miR-370-3p were significantly downregulated, while hsa-miR-1255b-5p was significantly upregulated in EOS (Figure 1E). These results confirmed that 8 of the 10 circRNAs and 3 miRNAs identified through high-throughput sequencing were present in the blood plasma of EOS patients, with consistent expression trends.

Circular Structural Verification of Screened circRNAs in Early-Onset Schizophrenia

Structural validation was performed for the 8 circRNAs that exhibited expression trends consistent with high-throughput sequencing data. The RNase R resistance assay demonstrated that the internal reference gene GAPDH, a linear RNA, showed a 931.724-fold reduction in expression after RNase R treatment. Significant changes in expression levels were observed for chr18:44526020–44526886+ and chr16:239999829–24046868+ following RNase R treatment, whereas minimal changes were detected for the other 6 circRNAs (Figure 2A). Sanger sequencing data further validated that 6 of the circRNAs—chr11:-33307959–33309057+, chr17:26490569–26499644+, chr19:41847788–41848152-, chr7:152007051–152012423-, chr12:-46622936–46648719- and chr16:68224671–68225678+—contained the expected circular junction sequences (Figure 2B–G). These findings confirmed that these 6 circRNAs were resistant to RNase R and possessed circular structures.

Construction of the Regulatory Axis Comprising Hsa-Circ-0000713, Hsa-miR-370-3p, Targets ANK3 and MGLL

Using literature reviews and structural validation data, we focused on genes associated with neuropsychiatric disorders and explored their binding relationships through dual-luciferase reporter assays. The results showed no binding relationship between hsa-circ-0000284 and hsa-miR-1255b-5p (Figure 3A). However, hsa-circ-0000713 contained a response element for hsa-miR-370-3p (Figure 3B). For hsa-miR-370-3p, identified as an intermediary in the ceRNA regulatory network, target predictions were performed using miRDB (http://www.mirdb.org/) and TargetScan (http://www.targetscan.org/vert_72/). Potential target genes included ankyrin-3 (ANK3), monoglyceride lipase (MGLL), and diacylglycerol kinase zeta (DGKZ). Co-transfection of wild-type (WT) ANK3 and hsa-miR-370-3p mimic significantly reduced luciferase activity, confirming a targeted binding relationship (Figure 3C). Similarly, hsa-miR-370-3p showed binding to the 3'UTR of MGLL (Figure 3D), but no such relationship was observed with DGKZ (Figure 3E). These results indicated that hsa-circ-0000713 contained a response element for hsa-miR-370-3p, which, in turn, exhibited targeted binding relationships with ANK3 and MGLL.

To explore the regulatory relationships among the molecules involved in binding interactions, an overexpression plasmid and two siRNAs targeting hsa-circ-0000713 were constructed. In the overexpression group, hsa-circ-0000713 expression was significantly upregulated compared with the blank vector group. This upregulation resulted in a significant downregulation of hsa-miR-370-3p and upregulation of the target genes ANK3 and MGLL (Figure 3F). Of the two siRNAs, si-2-hsa-circ-0000713 effectively knocked down the expression of the target gene (Figure 3G). Compared with the control, hsa-miR-370-3p was significantly upregulated in the si-2-hsa-circ-0000713 group, while ANK3 and MGLL expression levels were significantly downregulated (Figure 3H). These results indicated that hsa-circ-0000713 was negatively correlated with hsa-

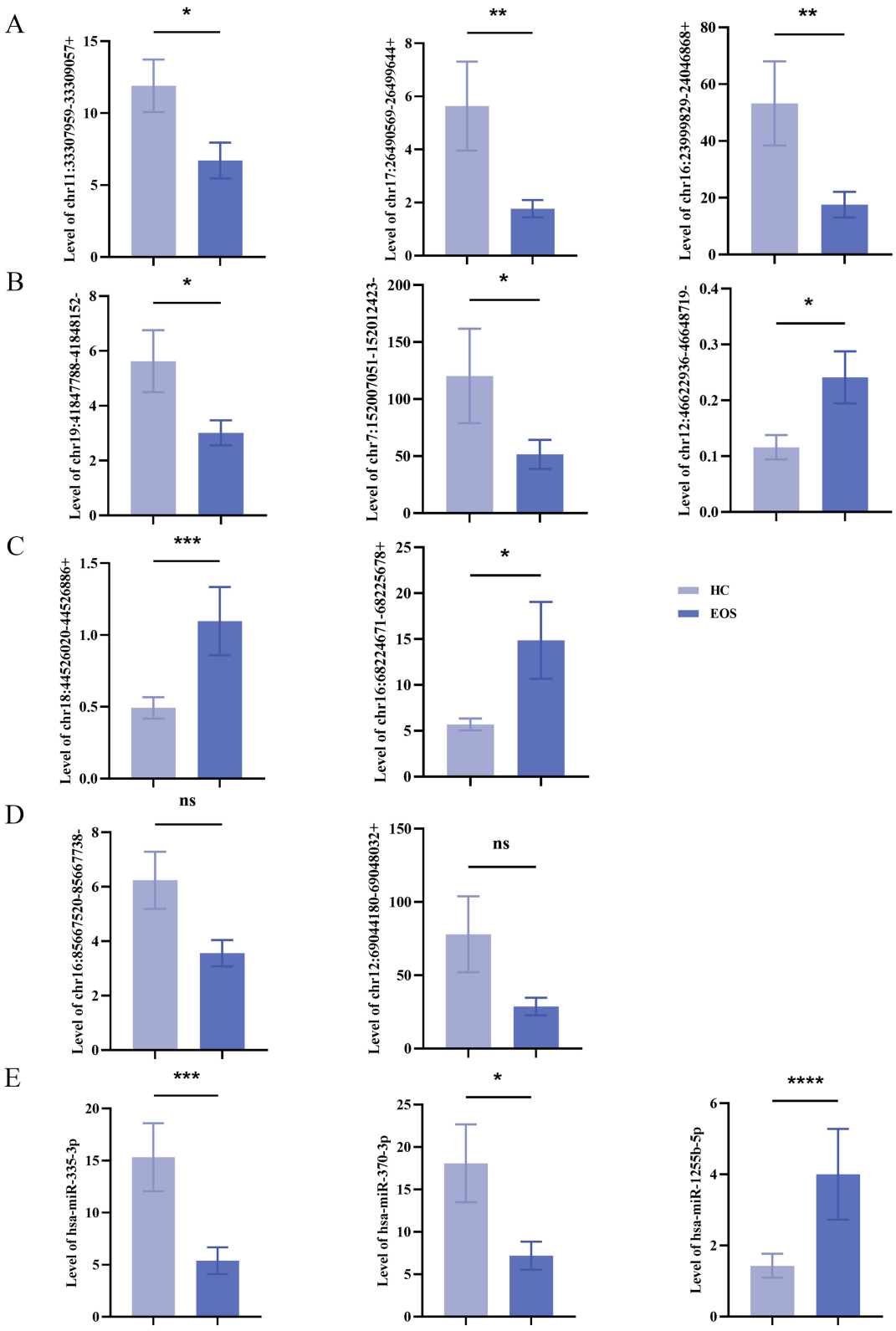

Figure 1 Expressed validation of selected circRNAs and miRNAs in peripheral blood plasma samples from patients with EOS. (**A**–**C**) Chr11: 33,307,959–33,309,057+ (*P*=0.0198), chr17:26,490,569–26,499,644+ (*P*=0.0040), chr16:23,999,829–24,046,868+ (*P*=0.0024), chr19:41,847,788–41,848,152- (*P*=0.0112), and chr7:152007051—152,012,423- (*P*=0.0219) were significantly downregulated, while chr12:46,622,936–46,648,719- (*P*=0.0401), chr18:44,526,020–44,526,886+ (*P*=0.0008), chr16:68,224,671-–68,225,678+ (*P*=0.0280) were significantly upregulated. (**D**) Expressions of chr16:85,667,520–85,667,738- (*P*=0.0503) and chr12:69,044,180–69,048,032+ (*P*=0.0969) were not statistically significant. (**E**) Hsa-miR-335-3p (*P*=0.0005), hsa-miR-370-3p (*P*=0.0248) were significantly downregulated, and hsa-miR-1255b-5p (*P*<0.0001) was significantly upregulated (HCs=29, healthy control group; EOS=32, early-onset schizophrenia group; ns, not statistically significant; **P*<0.05, ***P*<0.01, ****P*<0.001, *****P*<0.0001).

https://doi.org/10.2147/NDT.S521634

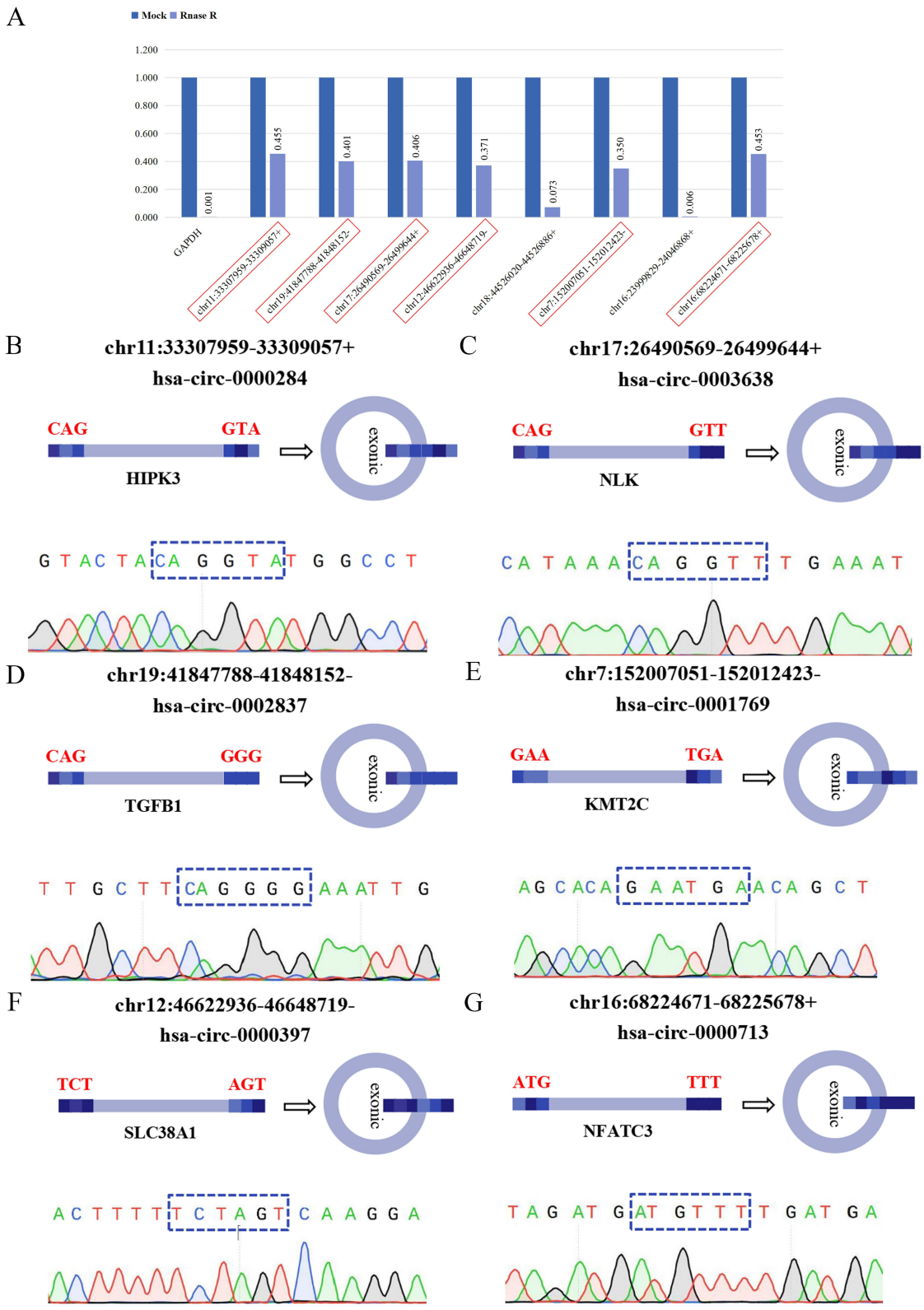

Figure 2 Structural verification of screened circRNAs through RNase R resistance assay and Sanger sequencing. (**A**) After RNase R treatment, the expression of the reference gene GAPDH exhibited a large fold change, with the pre-treatment level being 931.724 times that of the post-treatment level. The fold changes for the genes chr11:33307959-–33309057+ (2.198 times), chr19:41847788–41848152- (2.492 times), chr17:26490569–26499644+ (2.465 times), chr12:46622936–46648719- (2.693 times), chr7:152007051-–152012423- (2.861 times), and chr16:68224671–68225678+ (2.208 times) were modest. The fold changes for the genes chr18:44526020–44526886+ (13.789 times) and chr16:23999829–24046868+ (156.891 times) were large. (**B–G**) The cloned sequences of chr11:33307959–33309057+ (CAGGTA), chr17:26490569–26499644+ (CAGGTT), chr19:41847788–41848152- (CAGGGG), chr7:152007051–152012423- (GAATGA), chr12:46622936–46648719- (TCTAGT), and chr16:68224,671–68225678+ (ATGTTT) had corresponding back-spliced junction sites.

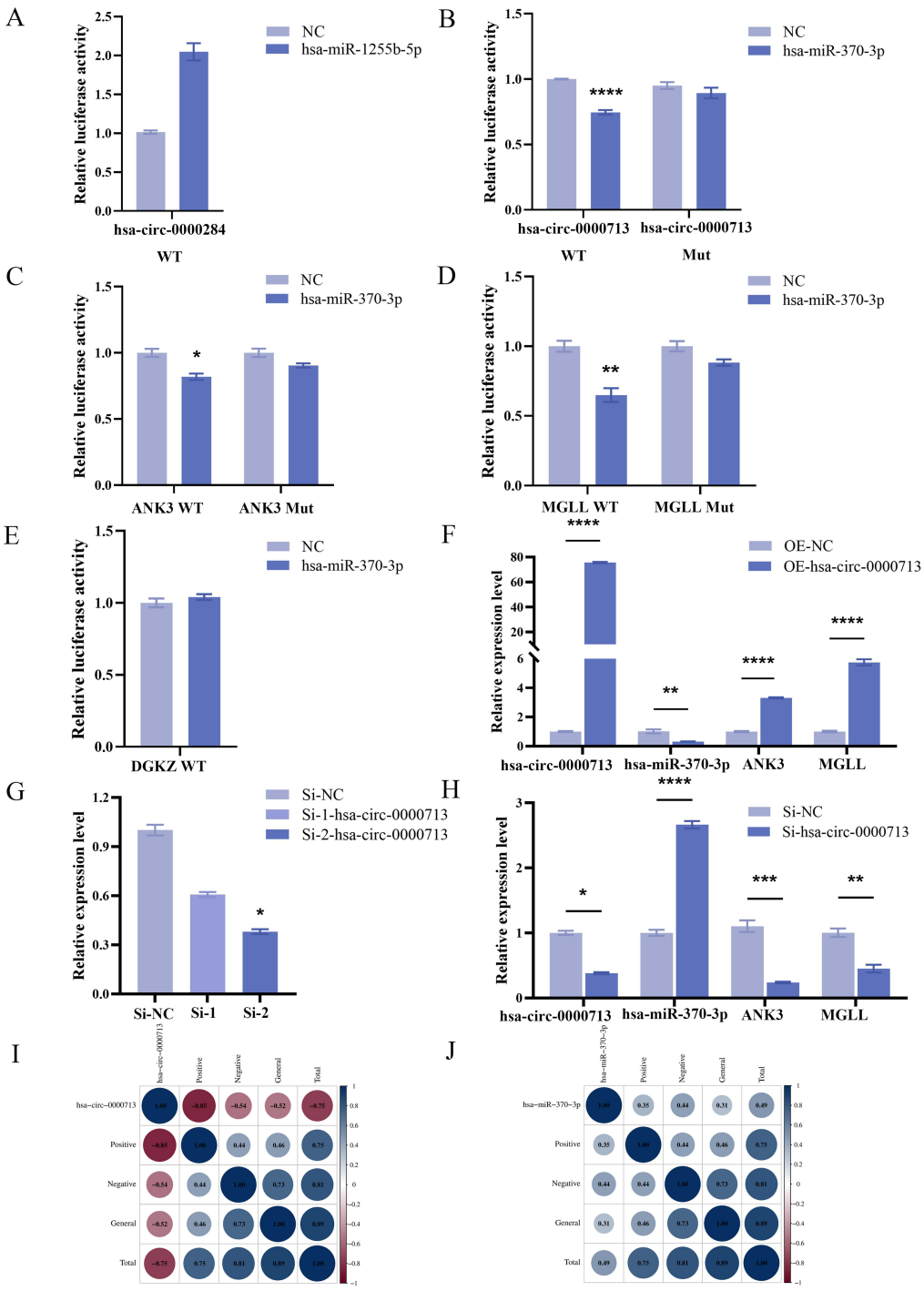

Figure 3 Construction of the multi-molecular regulatory axis comprising hsa-circ-0000713, hsa-miR-370-3p, targets ANK3 and MGLL. (**A**) Compared to co-transfection of hsa-circ-0000284 WT and NC mimic, luciferase activity was increased when co-transfecting hsa-circ-0000284 WT and hsa-miR-1255b-5p mimic. (**B**) Co-transfection of hsa-circ-0000713 WT and hsa-miR-370-3p mimic resulted in a significant downregulation of luciferase activity (P<0.0001). There was no significant decrease in luciferase activity when co-transfecting hsa-circ-0000713 Mut and hsa-miR-370-3p mimic (P>0.9999). (**C**) Co-transfection of ANK3 WT and hsa-miR-370-3p mimic resulted in a significant downregulation of luciferase activity (P=0.0395). There was no significant decrease in luciferase activity when co-transfecting ANK3 Mut and hsa-miR-370-3p mimic (P>0.9999). (**D**) Co-transfection of MGLL WT and hsa-miR-370-3p mimic resulted in a significant downregulation of luciferase activity (P=0.0052). There was no significant decrease in luciferase activity when co-transfecting MGLL Mut and hsa-miR-370-3p mimic (P=0.1000). (**E**) Compared to co-transfection of DGKZ WT and NC mimic, luciferase activity was increased when co-transfecting DGKZ WT and hsa-miR-370-3p mimic. (**F**) Compared to the NC group, the overexpression group showed the statistically significant upregulation of hsa-circ-0000713 (P<0.0001), ANK3 (P<0.0001), MGLL (P<0.0001) and a statistically significant downregulation of hsa-miR-370-3p (P=0.0064). (**G**) Compared to the Si-NC, hsa-circ-0000713 was downregulated without statistical significance in the Si-1-hsa-circ-0000713 transfected group (P=0.5391) and significantly downregulated in the Si-2-hsa-circ-0000713 transfected group (P=0.0219). (**H**) Compared to the NC group, the Si-2-hsa-circ-0000713 group showed the statistically significant downregulation of hsa-circ-0000713 (P=0.0219), ANK3 (P=0.0007), MGLL (P=0.0033) and a statistically significant upregulation of hsa-miR-370-3p. (**I**) Hsa-circ-0000713 was significantly correlated with positive symptoms (r=−0.85, P=0.0005) and total score (r=−0.75, P=0.005). (**J**) Hsa-miR-370-3p was significantly correlated with negative symptoms (r=0.44, P=0.048) and total score (r=0.49, P=0.003; P<0.0001; **P*<0.05, ***P*<0.01, ****P*<0.001, *****P*<0.0001).

https://doi.org/10.2147/NDT.S521634

miR-370-3p and positively correlated with ANK3 and MGLL. Conversely, hsa-miR-370-3p negatively regulated the expression levels of ANK3 and MGLL. These findings suggested that hsa-circ-0000713 functioned as a molecular sponge, mitigating the inhibitory effects of hsa-miR-370-3p on ANK3 and MGLL.

To further explore the correlation between the expression levels of core genes and the severity of clinical symptoms in patients with EOS, we used the PANSS scale to assess positive symptoms, negative symptoms, and general pathological symptoms, treating each score as a continuous variable. Spearman correlation analysis showed that the expression level of hsa-circ-0000713 was significantly negatively correlated with positive symptoms (r=−0.85, *P*=0.0005) and total score (r=−0.75, *P*=0.005). The expression level of hsa-miR-370-3p was significantly positively correlated with negative symptoms (r=0.44, *P*=0.048) and total score (r=0.49, *P*=0.003, Figure 3I and J).

Brain Validation of the circRNAs-miRNAs-mRNAs Regulatory Axis in Early-Onset Schizophrenia

Behavioral analysis of the MAM and PolyI:C models showed significantly increased total movement distance and velocity compared to HCs, indicative of heightened activity, restlessness, and exacerbated anxiety-like behaviors associated with elevated stress levels (Figure 4A and B). Additionally, the new object recognition index was significantly decreased in the MAM and PolyI:C models, suggesting impaired perception and memory of novel objects (Figure 4C). A significant reduction in spontaneous alternation accuracy in these models indicated impaired spatial working memory in SD rats (Figure 4D).

Brain tissues from HCs and the MAM and PolyI:C models were collected for further analysis. In the prefrontal cortex of the MAM and PolyI:C models, hsa-circ-0000713 expression was significantly increased, while hsa-miR-370-3p expression was significantly decreased (Figure 4E and F). Similarly, ANK3 and MGLL expression levels were significantly elevated in the prefrontal cortex of these models (Figure 4G and H). These results were consistent with findings from the peripheral blood plasma samples of EOS patients. Hsa-circ-0000713 acted as a sponge for hsa-miR-370-3p, reducing its inhibitory effects on ANK3 and MGLL. These findings suggested that the hsa-circ-0000713–hsa-miR-370-3p–ANK3/MGLL regulatory axis may contribute to EOS pathogenesis by mediating abnormal development of the prefrontal cortex (Figure 4I).

Discussion

Based on our research group's previous high-throughput sequencing datasets of circRNAs and miRNAs,[22] this study identified eight circRNAs and three miRNAs with significant and stable differential expression in the validation cohort, comprising 32 EOS patients and 29 HCs. Among these, six circRNAs were confirmed to contain trans-splicing sites. Through a combination of dual-luciferase reporter assays, cell knockdown, and overexpression experiments, a specific multi-molecular regulatory axis in EOS was identified. Specifically, hsa-circ-0000713 functioned as a molecular sponge for hsa-miR-370-3p, alleviating its inhibitory effects on the target genes ANK3 and MGLL. The expression level of hsa-circ-0000713 showed a significant negative correlation with patients' positive symptoms (r=−0.85) and the total score (r=−0.75), suggesting that it might exert the inhibitory effect in the pathological process of positive symptoms in EOS and has the potential to serve as a specific biomarker for positive symptoms of the disorder. The expression level of hsa-miR-370-3p displayed a significant positive correlation with negative symptoms (r=0.44) and the total score (r=0.49), indicating that it might play a promoting role in the pathological progression of negative symptoms. The lower correlation coefficient of hsa-miR-370-3p compared to that of hsa-circ-0000713 implies a weaker association with negative symptoms, potentially reflecting the heterogeneity of negative symptoms in patients or the indirect role of hsa-miR-370-3p.

The initiating gene of this regulatory axis, hsa-circ-0000713, originates from the reverse splicing of the activated T nuclear factor 3 (NFATC3), and is thus designated as hsa-circ-NFATC3. Dysfunction of NFATC3 in response to SZ risk factors, particularly stress, compromises its typical roles in mediating electrophysiological processes, immune responses, and neuroprotective mechanisms. This dysfunction occurs through its participation in a complex bioprotein cascade involving several other genes implicated in SZ susceptibility. Over time, the cumulative impact of this dysfunction

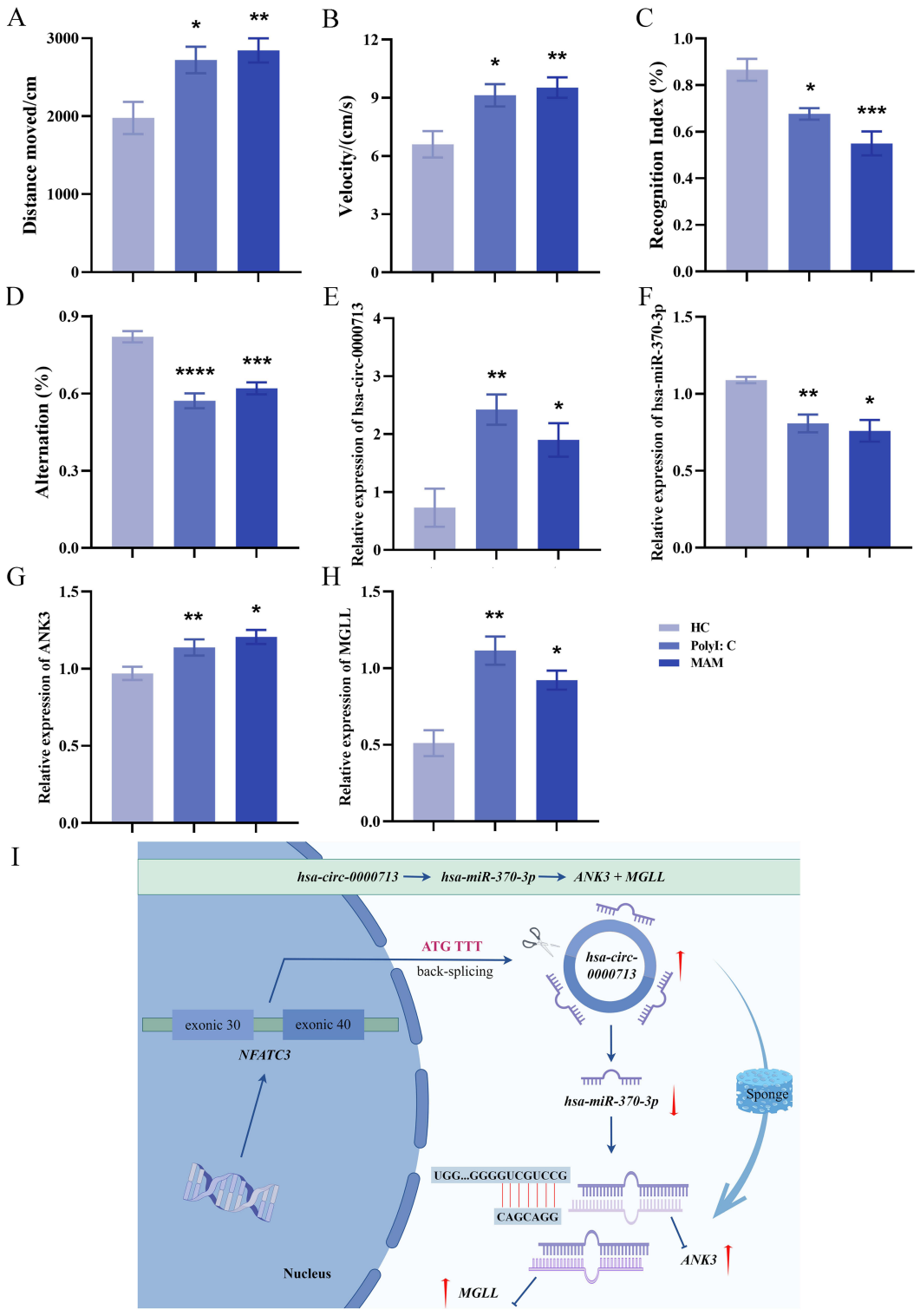

Figure 4 Brain validation of the hsa-circ-0000713-hsa-miR-370-3p-ANK3/MGLL axis in MAM and PolyI: C. (**A**) Compared to the control group, the total movement distance of the MAM and PolyI:C model groups were significantly increased (HC vs MAM: P=0.0097, HC vs PolyI:C: P=0.0253). (**B**) Compared to the control group, the velocity of the MAM and PolyI: C model groups were significantly increased (HC vs MAM: P=0.0092, HC vs PolyI:C: P=0.0233). (**C**) Compared to the control group, the recognition index of the MAM and PolyI:C model groups were significantly decreased (HC vs MAM: P=0.0003, HC vs PolyI:C: P=0.0178). (**D**) Compared to the control group, the alternation of the MAM and PolyI:C model groups were significantly decreased (HC vs MAM: P=0.0001, HC vs PolyI:C: P<0.0001). (**E**) Compared to the control group, hsa-circ-0000713 was significantly increased in the prefrontal cortex of MAM (P=0.0441) and PolyI:C models (P=0.0094). (**F**) Compared to the control group, hsa-miR-370-3p was significantly decreased in the prefrontal cortex of MAM (P=0.0119) and PolyI:C models (P=0.0099). (**G**) Compared to the control group, ANK3 was significantly increased in the prefrontal cortex of MAM (P=0.0139) and PolyI:C models (P=0.0079). (**H**) Compared to the control group, MGLL was significantly increased in the prefrontal cortex of MAM (P=0.0170) and PolyI:C models (P=0.0055). (**I**) hsa-circ-0000713 could act as a sponge for hsa-miR-370-3p, reducing the inhibitory effects of hsa-miR-370-3p on the target ANK3 and MGLL (The red coloured upwards and downwards arrows indicate upregulation and downregulation of gene expression levels, respectively. **P*<0.05, ***P*<0.01, ****P*<0.001, *****P*<0.0001).

https://doi.org/10.2147/NDT.S521634

manifests as the characteristic symptoms of SZ.[30] Furthermore, NFATC3, as the downstream transcription factor and output of the non-classical Wnt/Ca^{2+} pathway, has been shown to be significantly increased in SZ.[31] Hsa-miR-370-3p plays a regulatory role in various biological processes. It inhibits the invasion and migration of trophoblast cells by downregulating CDC25B, thereby influencing fetal growth regulation.[32] Additionally, it modulates the proliferation, invasion, angiogenesis, glutamine metabolism, and apoptosis of ovarian cancer cells, effectively suppressing tumor growth in vivo.[33]

The target gene ANK3 encodes the Ankyrin-G protein, which plays a critical role in cell localization, the induction of nerve cell development, and the regulation of synaptic plasticity.[34] Variations in the ANK3 can influence the number of inhibitory synapses in the forebrain, resulting in significant deficits in executive function and visual memory, as well as an elevated risk of bipolar disorder.[35–37] Additionally, patients with SZ carrying the polymorphic site rs10761482 of ANK3 exhibit substantial impairments in language comprehension, logical memory, and processing speed.[38] Another target gene, MGLL, encodes a crucial metabolic enzyme involved in various physiological processes. It plays a pivotal role in pain mediation through the hydrolysis of the endocannabinoid 2-arachidonoyl glycerol, thereby participating in nociceptive signaling.[39,40] In tumor cells, MGLL maintains distinct carcinogenic lipid signaling levels via its hydrolyzed products, which, in turn, fuel tumor progression and metastasis.[41]

By investigating the brain expression patterns of the genes within this axis in two animal models of disease, we found that the levels of hsa-circ-0000713, ANK3, and MGLL in the prefrontal cortex of MAM and PolyI:C models were significantly increased, while the expression levels of hsa-miR-370-3p were significantly decreased. These findings were consistent with the results observed in peripheral blood samples of patients with EOS. This specific multi-molecular regulatory axis, hsa-circ -0000713–hsa-miR-370-3p–ANK3/MGLL, may be involved in the pathogenesis of EOS by mediating abnormal development of the prefrontal cortex. Previous studies have shown that patients with EOS exhibit structural abnormalities in the prefrontal cortex, including reduced gray matter volume and decreased neuronal count.[42–44] These structural abnormalities may lead to impaired function of the prefrontal cortex, subsequently affecting patients' cognitive functions and emotional regulation abilities.[45,46] For instance, during working memory tasks, patients with EOS demonstrate decreased activity in the prefrontal cortex, which may be associated with the recruitment of cognitive resources and task difficulty.[47]

The circRNAs-miRNAs-mRNAs regulatory networks have been shown to have diagnostic and therapeutic potential in various diseases. In Alzheimer disease (AD), rodent AD models and human intervention studies support the targeting of miRNAs to block the production of β-amyloid, inhibit the excessive phosphorylation of tau protein, and reduce neuroinflammation, providing a new perspective for diagnosis of AD.[48] Previous studies on circRNAs and miRNAs in cancer diagnosis is more mature. Multiple molecular axes related to the proliferation and migration of tumors were found, especially in the fields of lung cancer, hepatocellular carcinoma and breast cancer.[49–51] In the cardiovascular diseases, circRNA HRCR could be used as a diagnostic marker for coronary heart disease by binding to miR-223 to inhibit myocardial hypertrophy, and circOGDH could be used as a non-invasive marker for ischemic stroke by binding to miR-5112 to regulate brain injury.[52,53] CircRNAs and miRNAs have shown great potential in disease diagnosis, but clinical translation still faces challenges. Disease symptoms are highly heterogeneous, and most studies are based on single-center, small-sample data, lacking multi-center and large-sample verification. The diagnostic specificity of a single circRNA or miRNA for the disease is also limited. In order to improve accuracy, the development of the multi-marker combination is needed. The cost of circRNA detection technology is high and the degree of standardization is low. The low abundance of circRNA increases the difficulty of detection. The concentration fluctuation of miRNAs in body fluids and the separation efficiency of exosomes will affect the stability of detection. In the future, we can work hard in the above directions to promote the clinical application of circRNAs and miRNAs in disease diagnosis.

We analyzed the existence of targeted binding interactions among circRNAs-miRNAs-mRNAs in EOS, explored the regulatory relationships between molecules on this axis, and investigated the expression patterns of these genes in the plasma of patients with EOS and brain tissue from animal models. However, there are several limitations. This study mainly evaluated the autonomic behavior, anxiety, cognitive function, and spatial recognition memory phenotype of the SZ-like models through open field test, novel object recognition, and Y-maze alternating behavior test. Prepulse inhibition testing has high value in verifying the fidelity of SZ-like models, and should be included in the behavioral paradigm of our research. MK-801 is a classic modeling method based on the hypothesis of glutamate dysfunction in SZ.

Given the highly conserved multi-molecular axis observed in this study, which exhibit good reproducibility in MAM and Poly I:C SZ models related to abnormal neural development and immune activation. Previous literatures showed that the N-methyl-D-aspartic acid (NMDA) receptors in both MAM and Polyl:C rat models exhibit dysfunction, which is consistent with the glutamate deficiency in the MK-801 model.[54,55] In the next stage, we will investigate whether the axis identified in this study operates through similar mechanisms within the MK-801 model. In addition, our study shows that this axis may be involved in the pathogenesis of SZ by mediating abnormal development of the prefrontal cortex. The next stage should be to intervene in vivo to normalize the expression of these genes and observe whether these can alleviate the behavioral phenotype of SZ. Moreover, the striatum is a key region of dopamine system abnormalities in SZ, which is closely related to positive symptoms and cognitive function. Literature review showed that ANK3 may affect the striatum-cortical circuit by regulating synaptic proteins or ion channels, and MGLL regulates dopamine signaling in the striatum by degrading the endogenous cannabinoid 2-monoacylglycerol.[56,57] Therefore, in the next animal experiments, we will further focus on the expression changes of these genes in the striatum, and explore whether there is a synergistic effect between the striatum and prefrontal cortex and how it works.

Conclusions

In summary, we identified a specific multi-molecular regulatory axis, hsa-circ-0000713–hsa-miR-370-3p–ANK3/MGLL, which may play a role in the pathogenesis and development of EOS by mediating abnormal prefrontal cortex development. These findings provide valuable insights to deepen the understanding of the pathological mechanisms of EOS and enrich the content for auxiliary objective diagnosis of the disorder.

Data Sharing Statement

High-throughput sequencing datasets of circRNAs and miRNAs related to early-onset schizophrenia can be downloaded from the GEO database (from the corresponding author of this manuscript, Sha Liu): https://www.ncbi.nlm.nih.gov/geo/query/acc.cgi?acc=GSE280722 and https://www.ncbi.nlm.nih.gov/geo/query/acc.cgi?acc=GSE280723. After the publication of the manuscript, individual deidentified participant data (including basic information, health records, examination results, and diagnostic information) and Supplementary Material can be obtained by emailing the corresponding author.

Ethics Approval and Informed Consent

The study was conducted according to the guidelines of the Declaration of Helsinki, and approved by the Ethics Committee of First Hospital of Shanxi Medical University (China Clinical Trial Registry: ChiCTR1900025838). The care of laboratory animals involved in this study was in accordance with the guidelines of Experimental Animal Center of Shanxi Medical University (2021-150).

Consent for Publication

The authors declare that the details of any images, recordings, etc involved in this manuscript can be published.

Acknowledgments

We would like to thank the members of Shanxi Key Laboratory of Artificial Intelligence Assisted Diagnosis and Treatment for Mental Disorder for their helpful discussion and technical support. This study was supported by the the National Natural Science Foundation of China (82371511, 82271546), Shanxi Provincial Department of Education Shanxi Provincial University of Higher Science and Technology Innovation Project (2022L228), Shanxi Federation of Social Sciences and Shanxi Association of Experts and Scholars 2023-2024 High-quality Development Research Project of Shanxi Province Research Project Cultivation Project (DJKZXKT2023282). Special Fund for Science and Technology Innovation Teams of Shanxi Province (202304051001049); Fund Program for the Scientific Activities of Selected Returned Overseas Professionals in Shanxi Province (20240041); Shanxi Province Higher Education "Billion Project" Science and Technology Guidance Project (BYJL062).

Disclosure

The authors declare that they have no financial and non-financial competing interests in this work.

References

1. Siris SG. Suicide and schizophrenia. *J Psychopharmacol*. 2001;15(2):127–135. doi:10.1177/026988110101500209
2. Xiao H, Zhu W, Jing D. Association between frailty and common psychiatric disorders: a bidirectional Mendelian randomization study. *J Affect Disord*. 2025;371:1–5. doi:10.1016/j.jad.2024.11.041
3. Moura BM, van Rooijen G, Schirmbeck F, et al. A network of psychopathological, cognitive, and motor symptoms in schizophrenia spectrum disorders. *Schizophr Bull*. 2021;47(4):915–926. doi:10.1093/schbul/sbab002
4. Hall H. Dissociation and misdiagnosis of schizophrenia in populations experiencing chronic discrimination and social defeat. *J Trauma Dissociation*. 2024;25(3):334–348. doi:10.1080/15299732.2022.2120154
5. Li C, Wang Z, Zhang J, et al. Crosstalk of mRNA, miRNA, lncRNA, and circRNA and their regulatory pattern in pulmonary fibrosis. *Mol Ther Nucleic Acids*. 2019;18:204–218. doi:10.1016/j.omtn.2019.08.018
6. Kirby E, Tse WH, Patel D, Keijzer R. First steps in the development of a liquid biopsy in situ hybridization protocol to determine circular RNA biomarkers in rat biofluids. *Pediatr Surg Int*. 2019;35(12):1329–1338. doi:10.1007/s00383-019-04558-2
7. Vo JN, Cieslik M, Zhang Y, et al. The landscape of circular RNA in cancer. *Cell*. 2019;176(4):869–881.e13. doi:10.1016/j.cell.2018.12.021
8. Werfel S, Nothjunge S, Schwarzmayr T, Strom TM, Meitinger T, Engelhardt S. Characterization of circular RNAs in human, mouse and rat hearts. *J Mol Cell Cardiol*. 2016;98:103–107. doi:10.1016/j.yjmcc.2016.07.007
9. Zimmerman AJ, Hafez AK, Amoah SK, et al. A psychiatric disease-related circular RNA controls synaptic gene expression and cognition. *Mol Psychiatry*. 2020;25(11):2712–2727. doi:10.1038/s41380-020-0653-4
10. Holdt LM, Kohlmaier A, Teupser D. Molecular roles and function of circular RNAs in eukaryotic cells. *Cell Mol Life Sci*. 2018;75(6):1071–1098. doi:10.1007/s00018-017-2688-5
11. Li X, Yang L, Chen LL. The biogenesis, functions, and challenges of circular RNAs. *Mol Cell*. 2018;71(3):428–442. doi:10.1016/j.molcel.2018.06.034
12. Piwecka M, Glažar P, Hernandez-Miranda LR, et al. Loss of a mammalian circular RNA locus causes miRNA deregulation and affects brain function. *Science*. 2017;357(6357):eaam8526.
13. He K, Guo C, He L, Shi Y. MiRNAs of peripheral blood as the biomarker of schizophrenia. *Hereditas*. 2018;155:9. doi:10.1186/s41065-017-0044-2
14. Smith B, Treadwell J, Zhang D, et al. Large-scale expression analysis reveals distinct microRNA profiles at different stages of human neurodevelopment. *PLoS One*. 2010;5(6):e11109. doi:10.1371/journal.pone.0011109
15. Perkins DO, Jeffries CD, Jarskog LF, et al. microRNA expression in the prefrontal cortex of individuals with schizophrenia and schizoaffective disorder. *Genome Biol*. 2007;8(2):R27. doi:10.1186/gb-2007-8-2-r27
16. Rybak-Wolf A, Stottmeister C, Glažar P, et al. Circular RNAs in the mammalian brain are highly abundant, conserved, and dynamically expressed. *Mol Cell*. 2015;58(5):870–885. doi:10.1016/j.molcel.2015.03.027
17. Li Z, Liu S, Li X, Zhao W, Li J, Xu Y. Circular RNA in schizophrenia and depression. *Front Psychiatry*. 2020;11:392. doi:10.3389/fpsyt.2020.00392
18. Tan G, Wang L, Liu Y, Zhang H, Feng W, Liu Z. The alterations of circular RNA expression in plasma exosomes from patients with schizophrenia. *J Cell Physiol*. 2021;236(1):458–467. doi:10.1002/jcp.29873
19. Xie M, Zhang Y, Yan L, Jin M, Lu X, Yu Q. Peripheral blood non-coding RNA as biomarker for schizophrenia: a review. *J Integr Neurosci*. 2024;23(2):42. doi:10.31083/j.jin2302042
20. Harvey RC, James AC, Shields GE. A systematic review and network meta-analysis to assess the relative efficacy of antipsychotics for the treatment of positive and negative symptoms in early-onset schizophrenia. *CNS Drugs*. 2016;30(1):27–39. doi:10.1007/s40263-015-0308-1
21. Harvey PD, Isner EC. Cognition, social cognition, and functional capacity in early-onset schizophrenia. *Child Adolesc Psychiatr Clin N Am*. 2020;29(1):171–182. doi:10.1016/j.chc.2019.08.008
22. Li Z, Du X, Wang X, et al. The neurodevelopmental regulatory role and clinical value of hsa-circ-CORO1C-hsa-miR-708-3p-JARID2 + LNPEP axis in early-onset schizophrenia. *Schizophrenia*. 2024;10(1):119. doi:10.1038/s41537-024-00538-1
23. Gileta AF, Fitzpatrick CJ, Chitre AS, et al. Genetic characterization of outbred Sprague Dawley rats and utility for genome-wide association studies. *PLoS Genet*. 2022;18(5):e1010234. doi:10.1371/journal.pgen.1010234
24. Gulchina Y, Xu SJ, Snyder MA, Elefant F, Gao WJ. Epigenetic mechanisms underlying NMDA receptor hypofunction in the prefrontal cortex of juvenile animals in the MAM model for schizophrenia. *J Neurochem*. 2017;143(3):320–333. doi:10.1111/jnc.14101
25. Huo C, Liu X, Zhao J, Zhao T, Huang H, Ye H. Abnormalities in behaviour, histology and prefrontal cortical gene expression profiles relevant to schizophrenia in embryonic day 17 MAM-Exposed C57BL/6 mice. *Neuropharmacology*. 2018;140:287–301. doi:10.1016/j.neuropharm.2018.07.030
26. Khalil OS, Forrest CM, Pisar M, Smith RA, Darlington LG, Stone TW. Prenatal activation of maternal TLR3 receptors by viral-mimetic poly(I:C) modifies GluN2B expression in embryos and sonic hedgehog in offspring in the absence of kynurenine pathway activation. *Immunopharmacol Immunotoxicol*. 2013;35(5):581–593. doi:10.3109/08923973.2013.828745
27. Girardi CE, Zanta NC, Suchecki D. Neonatal stress-induced affective changes in adolescent Wistar rats: early signs of schizophrenia-like behavior. *Front Behav Neurosci*. 2014;8:319. doi:10.3389/fnbeh.2014.00319
28. Estaphan S, Curpăn AS, Khalifa D, et al. Combined low dose of ketamine and social isolation: a possible model of induced chronic schizophrenia-like symptoms in male albino rats. *Brain Sci*. 2021;11(7):917. doi:10.3390/brainsci11070917
29. Bator E, Latusz J, Głowacka U, Radaszkiewicz A, Mudlaff K, Maćkowiak M. Adolescent social isolation affects schizophrenia-like behavior in the MAM-E17 model of schizophrenia. *Neurotox Res*. 2018;34(2):305–323. doi:10.1007/s12640-018-9888-0
30. Marballi KK, Gallitano AL. Immediate early genes anchor a biological pathway of proteins required for memory formation, long-term depression and risk for schizophrenia. *Front Behav Neurosci*. 2018;12:23. doi:10.3389/fnbeh.2018.00023
31. Hoseth EZ, Krull F, Dieset I, et al. Exploring the Wnt signaling pathway in schizophrenia and bipolar disorder. *Transl Psychiatry*. 2018;8(1):55. doi:10.1038/s41398-018-0102-1
32. Huang Z, Zhu L, Zhang Q, Zhao D, Yao J. Circular RNA hsa-circ-0005238 enhances trophoblast migration, invasion and suppresses apoptosis via the miR-370-3p/CDC25B axis. *Front Med Lausanne*. 2022;9:943885. doi:10.3389/fmed.2022.943885

33. Ma H, Qu S, Zhai Y, Yang X. circ_0025033 promotes ovarian cancer development via regulating the hsa_miR-370-3p/SLC1A5 axis. *Cell Mol Biol Lett*. 2022;27(1):94. doi:10.1186/s11658-022-00364-2
34. Kloth K, Lozic B, Tagoe J, et al. ANK3 related neurodevelopmental disorders: expanding the spectrum of heterozygous loss-of-function variants. *Neurogenetics*. 2021;22(4):263–269. doi:10.1007/s10048-021-00655-4
35. Leussis MP, Berry-Scott EM, Saito M, et al. The ANK3 bipolar disorder gene regulates psychiatric-related behaviors that are modulated by lithium and stress. *Biol Psychiatry*. 2013;73(7):683–690. doi:10.1016/j.biopsych.2012.10.016
36. Roby Y. ANK3 gene polymorphisms and bipolar disorder: a meta-analysis. *Psychiatr Genet*. 2017;27(6):225–235. doi:10.1097/YPG.0000000000000186
37. Tang L, Liu J, Zhu Y, et al. ANK3 gene polymorphism Rs10994336 influences executive functions by modulating methylation in patients with bipolar disorder. *Front Neurosci*. 2021;15:682873. doi:10.3389/fnins.2021.682873
38. Zhong X, Zhang L, Han S, An Z, Yi Q. Case control study of association between the ANK3 rs10761482 polymorphism and schizophrenia in persons of Uyghur nationality living in Xinjiang China. *Shanghai Arch Psychiatry*. 2014;26(5):288–293. doi:10.11919/j.issn.1002-0829.214033
39. Clapper JR, Henry CL, Niphakis MJ, et al. Monoacylglycerol lipase inhibition in human and rodent systems supports clinical evaluation of endocannabinoid modulators. *J Pharmacol Exp Ther*. 2018;367(3):494–508. doi:10.1124/jpet.118.252296
40. Huang X, Huang X, Guo H, et al. Intermittent hypoxia-induced METTL3 downregulation facilitates MGLL-mediated lipolysis of adipocytes in OSAS. *Cell Death Discov*. 2022;8(1):352. doi:10.1038/s41420-022-01149-4
41. Zhang J, Song Y, Shi Q, Fu L. Research progress on FASN and MGLL in the regulation of abnormal lipid metabolism and the relationship between tumor invasion and metastasis. *Front Med*. 2021;15(5):649–656. doi:10.1007/s11684-021-0830-0
42. Gan JL, Cheng ZX, Duan HF, Yang JM, Zhu XQ, Gao CY. Atypical antipsychotic drug treatment for 6 months restores N-acetylaspartate in left prefrontal cortex and left thalamus of first-episode patients with early onset schizophrenia: a magnetic resonance spectroscopy study. *Psychiatry Res*. 2014;223(1):23–27. doi:10.1016/j.pscychresns.2014.04.010
43. Kolb B. Patricia Goldman-Rakic: a pioneer and leader in frontal lobe research. *Front Hum Neurosci*. 2023;17:1334264. doi:10.3389/fnhum.2023.1334264
44. Wang L, Liu R, Liao J, et al. Meta-analysis of structural and functional brain abnormalities in early-onset schizophrenia. *Front Psychiatry*. 2024;15:1465758. doi:10.3389/fpsyt.2024.1465758
45. Sakurai T, Gamo NJ. Cognitive functions associated with developing prefrontal cortex during adolescence and developmental neuropsychiatric disorders. *Neurobiol Dis*. 2019;131:104322. doi:10.1016/j.nbd.2018.11.007
46. Friedman NP, Robbins TW. The role of prefrontal cortex in cognitive control and executive function. *Neuropsychopharmacology*. 2022;47(1):72–89. doi:10.1038/s41386-021-01132-0
47. Kyriakopoulos M, Dima D, Roiser JP, Corrigall R, Barker GJ, Frangou S. Abnormal functional activation and connectivity in the working memory network in early-onset schizophrenia. *J Am Acad Child Adolesc Psychiatry*. 2012;51(9):911–20.e2. doi:10.1016/j.jaac.2012.06.020
48. Guo X. A state-of-the-art review on miRNA in prevention and treatment of Alzheimer's disease. *Zhejiang Da Xue Xue Bao Yi Xue Ban*. 2023;52(4):485–498. doi:10.3724/zdxbyxb-2023-0324
49. Liang ZZ, Guo C, Zou MM, Meng P, Zhang TT. circRNA-miRNA-mRNA regulatory network in human lung cancer: an update. *Cancer Cell Int*. 2020;20:173. doi:10.1186/s12935-020-01245-4
50. Zhao J, Zou H, Han C, Ma J, Zhao J, Tang J. Circlular RNA BARD1 (Hsa_circ_0001098) overexpression in breast cancer cells with TCDD treatment could promote cell apoptosis via miR-3942/BARD1 axis. *Cell Cycle*. 2018;17(24):2731–2744. doi:10.1080/15384101.2018.1556058
51. Han TS, Hur K, Cho HS, Ban HS. Epigenetic associations between lncRNA/circRNA and miRNA in hepatocellular carcinoma. *Cancers*. 2020;12(9):2622. doi:10.3390/cancers12092622
52. Lin F, Chen HW, Zhao GA, et al. Advances in research on the circRNA-miRNA-mRNA network in coronary Heart Disease Treated with Traditional Chinese Medicine. *Evid Based Complement Alternat Med*. 2020;2020:8048691. doi:10.1155/2020/8048691
53. Yuan L, Chen W, Xiang J, Deng Q, Hu Y, Li J. Advances of circRNA-miRNA-mRNA regulatory network in cerebral ischemia/reperfusion injury. *Exp Cell Res*. 2022;419(2):113302. doi:10.1016/j.yexcr.2022.113302
54. Romero-Miguel D, Casquero-Veiga M, MacDowell KS, et al. A characterization of the effects of minocycline treatment during adolescence on structural, metabolic, and oxidative stress parameters in a maternal immune stimulation model of neurodevelopmental brain disorders. *Int J Neuropsychopharmacol*. 2021;24(9):734–748. doi:10.1093/ijnp/pyab036
55. Tamaru M, Yoneda Y, Ogita K, Shimizu J, Matsutani T, Nagata Y. Excitatory amino acid receptors in brains of rats with methylazoxymethanol-induced microencephaly. *Neurosci Res*. 1992;14(1):13–25. doi:10.1016/s0168-0102(05)80003-3
56. Martín AB, Fernandez-Espejo E, Ferrer B, et al. Expression and function of CB1 receptor in the rat striatum: localization and effects on D1 and D2 dopamine receptor-mediated motor behaviors. *Neuropsychopharmacology*. 2008;33(7):1667–1679. doi:10.1038/sj.npp.1301558
57. Van Horn S, Driscoll H, Toufexis DJ. Transcriptomic dysregulation in animal models of attention-deficit hyperactivity disorder and nicotine dependence suggests shared neural mechanisms. *Brain Behav*. 2025;15(3):e70444. doi:10.1002/brb3.70444